Biochimica et Biophysica Acta 1833 (2013) 3218–3227

Contents lists available at ScienceDirect

Biochimica et Biophysica Acta

journal homepage: www.elsevier.com/locate/bbamcr

Aldehyde dehydrogenase-1a1 induces oncogene suppressor genes in B cell populations

R. Yasmeen [a], J.M. Meyers [a], C.E. Alvarez [b,c], J.L. Thomas [a], A. Bonnegarde-Bernard [d], H. Alder [e], T.L. Papenfuss [d], D.M. Benson Jr. [f], P.N. Boyaka [d], O. Ziouzenkova [a,*]

[a] Department of Human Sciences, The Ohio State University, Columbus, OH 43210, USA
[b] Center for Molecular and Human Genetics, The Research Institute at Nationwide Children's Hospital, Columbus, OH 43205, USA
[c] Department of Pediatrics, The Ohio State University College of Medicine, Columbus, OH 43210, USA
[d] Department of Veterinary Biosciences, The Ohio State University, Columbus, OH 43210, USA
[e] Nucleic Acid Shared Resource, Comprehensive Cancer Center, The Ohio State University, Columbus, OH 43210, USA
[f] Division of Hematology, Comprehensive Cancer Center, The Ohio State University, Columbus, OH 43210, USA

ARTICLE INFO

Article history:
Received 8 April 2013
Received in revised form 18 September 2013
Accepted 19 September 2013
Available online 27 September 2013

Keywords:
Homeobox transcription factor
Nuclear receptor
Retinaldehyde
Raldh1
Vitamin A metabolism
Multiple myeloma

ABSTRACT

The deregulation of B cell differentiation has been shown to contribute to autoimmune disorders, hematological cancers, and aging. We provide evidence that the retinoic acid-producing enzyme aldehyde dehydrogenase 1a1 (*Aldh1a1*) is an oncogene suppressor in specific splenic IgG1$^+$/CD19$^-$ and IgG1$^+$/CD19$^+$ B cell populations. *Aldh1a1* regulated transcription factors during B cell differentiation in a sequential manner: 1) retinoic acid receptor alpha (*Rara*) in IgG1$^+$/CD19$^-$ and 2) zinc finger protein *Zfp423* and peroxisome proliferator-activated receptor gamma (*Pparg*) in IgG1$^+$/CD19$^+$ splenocytes. In *Aldh1a1*$^{-/-}$ mice, splenic IgG1$^+$/CD19$^-$ and IgG1$^+$/CD19$^+$ B cells acquired expression of proto-oncogenic genes *c-Fos*, *c-Jun*, and *Hoxa10* that resulted in splenomegaly. Human multiple myeloma B cell lines also lack *Aldh1a1* expression; however, ectopic *Aldh1a1* expression rescued *Rara* and *Znf423* expressions in these cells. Our data highlight a mechanism by which an enzyme involved in vitamin A metabolism can improve B cell resistance to oncogenesis.

1. Introduction

The deregulation of B cell differentiation has been shown to play a causal role in autoimmune disorders, carcinogenesis, and aging [1]. B cells differentiate from B-lymphoid progenitors in the bone marrow and progress through many stages during differentiation to ultimately express B cell receptor (BCR). Lymphocytes expressing surface IgM migrate to the spleen [2], where self-reactive splenic B cells undergo apoptosis; others become responsive to T-cell-dependent and T-cell-independent antigens. The various B-cell populations are compartmentalized in different splenic zones, including red pulp, marginal zone, and white pulp. After pathogen exposure, they complete differentiation in germinal centers [2]. Specific populations of B cells can undergo alternative differentiation. For instance, purified mouse splenic B cells respond to stimulation with cytokines, anti-CD38, anti-CD40, anti-μ, and retinoic acid (RA) by enriching IgG1$^+$ and CD138$^+$ B cell populations and genes involved in the regulation of Ig somatic hypermutation and class switching [3]. In these B cells, RA contributed to the suppression of activation-induced deaminase (Aid), transcriptional regulators of differentiation (Pax5), and neoplastic transformation t(9;14) [3,4]. Oncogenic processes further diversify in B lymphoma cells [5]. The physiological mechanisms responsible for the formation of specific B cell subsets have remained unexplored.

The studies with dietary vitamin A (retinol or retinyl esters) highlighted a possible role for this pathway in specific B cell responses. Dietary vitamin A content influenced IgA production against T-cell dependent and T-cell independent type 2 antigens at mucosal locations [6]. Vitamin A deficiency in the diet diminishes immune responses and increases mortality [7–10]. These responses may be partially improved by supplementation with either vitamin A or its metabolite RA, arguing for RA as a mediator of these responses. The function of RA in B cell studies in vitro revealed that multiple aspects of B cell biology are RA-sensitive [10,11]. RA accelerated differentiation of a subset of proliferating lymphoid progenitor cells into B cells by targeting the oncogenes c-myc and cyclin D3, cytokines, and NFκB, as well as kinase p38/CDK2 [12,13]. RA treatment also promoted differentiation of malignant B cells, alone or in combination with rosiglitazone, an agonist for

Abbreviations: Aldh1a1, aldehyde dehydrogenase 1a1; AP1, activator protein 1 a heterodimeric transcription factor formed by *c-jun* and *c-fos*; c-Fos, transcription factor encoded by the FOS gene; c-Jun, protein encoded by *c-Jun* gene; *Hoxa10*, transcription factor homeobox protein a10; Ig, immunoglobulin; *Pparg*, peroxisome proliferator-activated receptor; RA, retinoic acid; *Rara*, retinoic acid receptor alpha; RARE, retinoic acid receptor response element; *Zfp423*, murine zinc finger protein; *Znf423*, human zinc finger protein

* Corresponding author at: 1787 Neil Avenue, 331A Campbell Hall, Columbus, OH 43210, USA. Tel.: +1 614 292 5034; fax: +1 614 292 8880.
E-mail address: ziouzenkova.1@osu.edu (O. Ziouzenkova).

0167-4889/$ – see front matter © 2013 Elsevier B.V. All rights reserved.
http://dx.doi.org/10.1016/j.bbamcr.2013.09.012

the nuclear receptor PPARγ [14]. The understanding of RA in immune function is incomplete. For example, a recent trial in Guinea–Bissau revealed a paradoxically higher mortality in girls supplemented with vitamin A than in placebo group [15]. In this study we dissected the role of endogenous vitamin A metabolism on gene regulation in B cells.

An increase in the intracellular RA concentrations is generated in response to various hormonal, dietary, and inflammatory stimuli and may be considered as a factor in endogenous differentiation of B cell subsets [11,16]. RA is produced sequentially. Alcohol dehydrogenases (ADH and SDR/RDH) oxidize retinol to retinaldehyde, which is dehydrogenated into RA by the members of aldehyde dehydrogenase-1 family of enzymes: ALDH1a1, ALDH1a2, and ALDH1a3 [17]. The principal mechanism of RA action is through the activation of RA receptors (RAR). RA binding to RAR induces its heterodimerization with retinoid X receptor, and binding to cognate response element (RARE) sequences in the promoters of target genes [18]. In addition, RA regulates a plethora of signaling and transcriptional pathways [19], including a *Zfp423*-dependent induction of *Pparg* expression [20]. Paracrine RA production by ALDH1 enzymes in dendritic cells plays an important role in B cell homing to the mucosa, and promotes IgA isotype class switching [21,22]. The role of RA-generating enzymes in B cells has remained unexplored. Here, we investigated the transcriptional function of ALDH1a1 in murine B cell subsets and in human multiple myeloma B cell lines.

2. Materials and methods

2.1. Reagents

We purchased reagents from Sigma-Aldrich (St. Louis, MO) and cell culture media from Invitrogen (Carlsbad, CA) unless otherwise indicated. Anti-mouse antibodies were: CD19 from BD Biosciences (San Jose, CA) and β-galactosidase from Abcam (Cambridge, MA).

2.2. Animal studies

All experimental protocols were approved by the Institutional Animal Care and User Committee. Water and regular chow (Harlan Laboratories, Indianapolis, IL) were available ad libitum in all mouse studies.

Study 1 employed Tg RARE-Hspa1b/lacZ (denoted as RARE-lacZ) reporter mice developed by Dr. J. Rossant using a transgenic construct containing 3 copies of the 32 bp RARE placed upstream of the mouse heat shock protein 1B promoter and β-galactosidase gene (lacZ) [23]. Female mice were purchased from the Jackson Laboratory (Bar Harbor, ME). Three RARE-lacZ and three wild-type C57BL/6J (WT) female mice (12–15 weeks old) were fed regular chow throughout this study.

Study 2: *Aldh1a1*$^{-/-}$ mice were previously generated in the laboratory of G. Duester [24] and characterized for their metabolic responses [20,25,26]. *Aldh1a1*$^{-/-}$ (n = 10) and WT (n = 9) 13–14 month old male and female mice were used for these studies. Mice were fed regular chow diet. Blood was collected by cardiac puncture in EDTA-containing tubes. The spleens isolated from 3 randomly-selected females were used for IgG1^{+}/CD19^{-} and IgG1^{+}/CD19^{+} B-cell separation. The remaining spleens and other organs were used for other analyses.

2.3. Human cells

Leukopacks (American Red Cross, Columbus, OH) were obtained from healthy donors under an Institutional Review Board-approved procurement protocol. Peripheral blood mononuclear cells (PBMC) were cultured in RPMI 1640 media (Invitrogen) supplemented with 10% fetal bovine serum (ICN Biomedicals, Irvine, CA) and kept at 37 °C in a 5% CO_2/air incubator.

2.4. Flow cytometry analysis (FACS)

Splenocyte suspension was obtained from whole spleens dissected from 4 WT and 4 *Aldh1a1*$^{-/-}$ mice (2 males and 2 females in each group). Briefly, spleens were collected and mononuclear cell suspensions were prepared by mechanical disruption with the aid of a cell strainer (BD Biosciences, San Jose, CA) followed by brief incubation in NH_4Cl (0.08%) to remove red blood cells. Splenocytes were resuspended in fluorescence-activated cell sorting buffer (FACS; PBS containing 0.1% BSA and 0.1% sodium azide) at 5×10^5/100 μL. Cells were stained with a panel of antibodies from AbD Serotec (Bio-Rad Laboratories, Inc., Hercules, CA) and available isotype controls. All antibodies were primary, non-conjugated with the exception of MHC class II which were directly conjugated to fluorescein isothiocyanate (FITC) and Alexa Fluor 647 (BD Biosciences), respectively. Secondary antibodies of either phycoerythrin (PE; 5 μL) or fluorescein isothiocyanate (FITC; 1 μL) were purchased from AbD Serotec and were used at various dilutions (1:10, 1:50, and 1:100) [27]. Samples were analyzed using BD Accuri flow cytometer and analyzed with BD Accuri Flow analysis software (BD Biosciences).

2.5. Purification of IgG1/CD19^{-} and IgG1/CD19^{+} B cells

Splenic B cell subsets were obtained from four WT and *Aldh1a1*$^{-/-}$ female and one male mice. They were purified by automated magnetic cell separation (autoMACS, Miltenyi Biotec). The cell suspensions were incubated with microbeads conjugated with anti-mouse CD19. The CD19^{-} and CD19^{+} populations were separated by autoMACS. The CD19^{-} and CD19^{+} fraction was further incubated with a biotinylated rat anti-mouse γ1 (clone G1-7.3, BD Biosciences) and streptavidin-conjugated microbeads. Populations of IgG1^{+}/CD19^{-} and IgG1^{+}/CD19^{+} were separated by autoMACS. Throughout, we denoted these populations as CD19^{-} and CD19^{+}. The purity (>98%) of the cell population was confirmed by FACS.

2.6. RNA isolation and quantitative real time PCR (qRT-PCR)

Total RNA was prepared using the RNeasy kit (Qiagen, Valencia, CA). qRT-PCR was performed with predesigned assays (Applied Biosystems, Foster City, CA) using a 7900HT Fast Real-Time PCR System, TaqMan detection system, and validated primers (Applied Biosystems, Foster City, CA) in triplicate as described [16]. The mRNA expression was calculated based on Tata-box binding protein (TBP) expression for normalization using the comparative Ct method.

2.7. NanoString gene expression profiling

The digital multiplexed NanoString nCounter mouse inflammation expression assay (NanoString Technologies) was performed with 100 ng of total RNA according to the manufacturer's instructions. RNA was isolated from CD19^{-} and CD19^{+} fraction isolated from 3 female WT and *Aldh1a1*$^{-/-}$ mice. NanoString's nCounter technology is based on direct detection of target molecules using color-coded molecular barcodes, providing a digital quantification of the number of target molecules [28]. Total mRNA (5 μL) was hybridized overnight with nCounter Reporter (20 μL) probes in hybridization buffer and nCounter Capture probes (5 μL). The hybridizations were incubated at 65 °C for 16–20 h in excess of probes to ensure that each target finds a probe pair. Excess probes were removed using two-step magnetic bead based purification on the nCounter Prep Station. The hybridization mixture containing target/probe complexes was allowed to bind to magnetic beads containing complementary sequences on the Capture Probe and washed followed by a sequential binding to sequences on the Reporter Probe. Biotinylated capture probe-bound samples were immobilized and recovered on a streptavidin-coated cartridge. The abundance of specific target molecules was then quantified using the nCounter Digital Analyzer to count

the individual fluorescent barcodes and assess target molecules present in each sample with a CCD camera. For each assay, a high-density scan (600 fields of view) was performed at the highest standard data resolution, 600 fields of view (FOV) that is the dynamic range and level of sensitivity in the system. Images were processed internally into a digital format and were normalized using the NanoString nSolver software analysis tool. Counts were normalized for all target RNAs in all samples based on the positive control RNA to account for differences in hybridization efficiency and post-hybridization processing, including purification and immobilization of complexes. Subsequently, a normalization of mRNA content was performed using six internal reference housekeeping genes that were included within the mouse inflammatory panel: *Cltc*, *Gapdh*, *Gusb*, *Hprt1*, *Pgk1*, and *Tubb*. The average was normalized by background counts for each sample obtained from the average of the eight negative control counts. Counts were corrected by subtracting the mean and 2 times standard deviation value of the negative control from the counts obtained for each target RNA.

2.8. Immunohistochemistry

Spleens and kidney were embedded in paraffin. Immunohistochemical analysis of spleens from WT and RARE-lacZ mice was performed with rabbit polyclonal β-galactosidase antibody (1:1000 dilution). Images were obtained using Olympus M081 IX50 and Pixera Viewfinder 3.0 software.

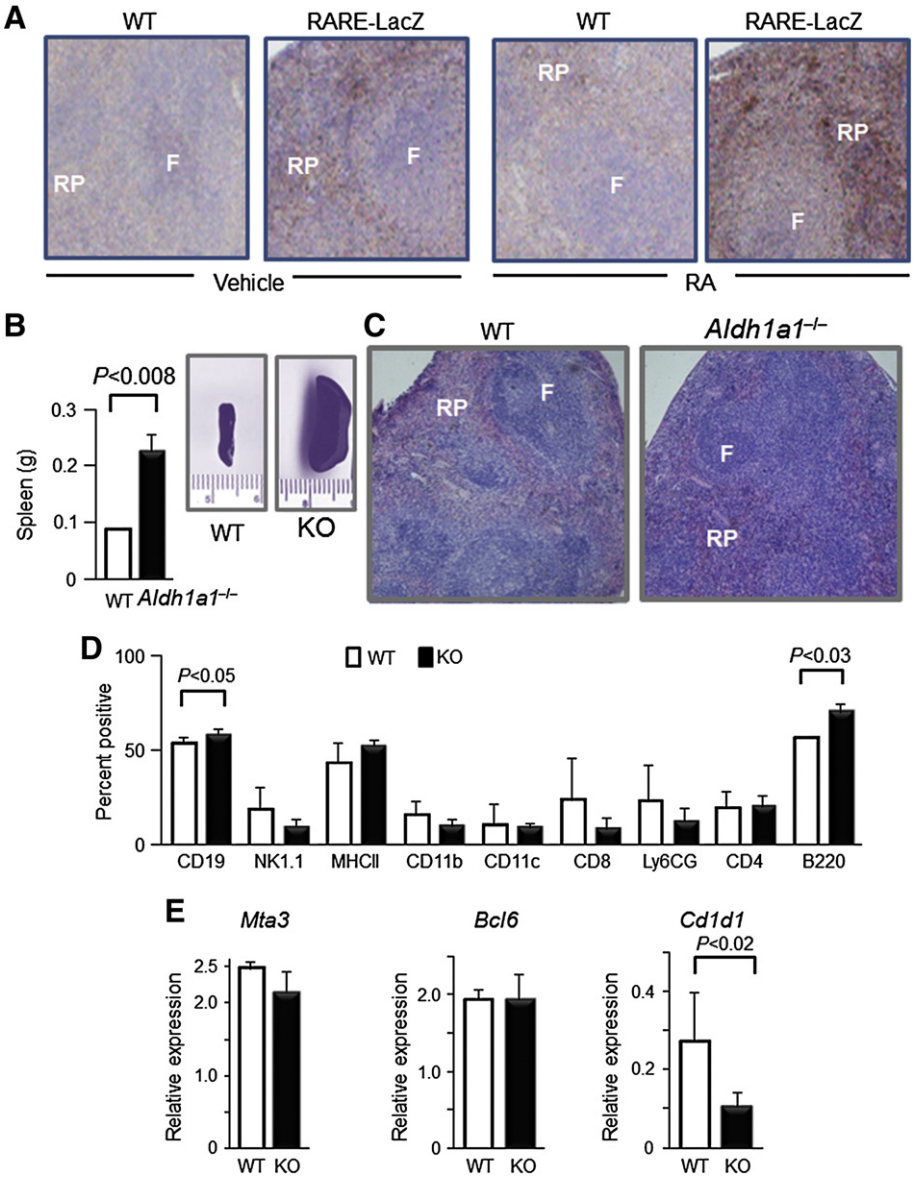

Fig. 1. Activation of retinoic acid receptor response element (RARE) accompanies splenic red pulp development, which depends on *Aldh1a1*. (A) RARE activation was studied in WT and RARE-LacZ mice (n = 3 from each group) which were injected every 48 h, up to a total of 3 injections with 1 mL PBS (vehicle) without or with RA (500 nM). RA was added into PBS from 500 μM RA stock solution in ethanol immediately before injection. Vehicle PBS solution contained 1 μL ethanol. All RA solutions were protected from light and stored under argon atmosphere. Total injected RA amount was 1.5 nmol per mouse (0.15 μg/dose). Immediately after the third injection, mice were harvested and their spleens were embedded in paraffin. Immunohistochemistry was performed with anti-β-galactosidase antibody. Heterogeneous brown β-galactosidase-positive areas were found in red pulp (RP) compared to follicular zone (F) (10× magnification). The RARE responses in adipose and hepatic tissues were described in [25]. (B) Weight of spleens (left panel, Study 2. *Aldh1a1*$^{-/-}$ (n = 10) and WT (n = 9)). Inset shows the representative whole spleen images of WT and *Aldh1a1*$^{-/-}$ mice. (C) Representative hematoxylin & eosin staining of paraffin embedded spleen section from WT and *Aldh1a1*$^{-/-}$ (KO) mice from the same study (n = 3 per group). (D) FACS analysis of splenocyte suspension isolated from whole spleens of *Aldh1a1*$^{-/-}$ (n = 4) and WT (n = 4) mice. *P*, significance levels, Mann–Whitney *U* test. (E) Expression of germinal center markers in the total spleen lysates isolated from WT (white bars) and *Aldh1a1*$^{-/-}$ (black bars) mice was analyzed by TaqMan assays (WT: n = 3; *Aldh1a1*$^{-/-}$ n = 5). Data were normalized by *TBP*. Significant difference was determined using Mann–Whitney *U* test.

2.9. Transfections

U266B1 (U266) and RPMI8226 were purchased from American Type Culture Collection (Manassas, VA), other B cell lines were provided by Dr. D.M. Benson, Jr. All human B cells were maintained in 15% fetal bovine serum/RPMI 1640 medium as previously described [29]. Human full length *Aldh1a1* cDNA expression vector was purchased from OriGene (Rockville, MD). U266 cells (6×10^6 per tube) were

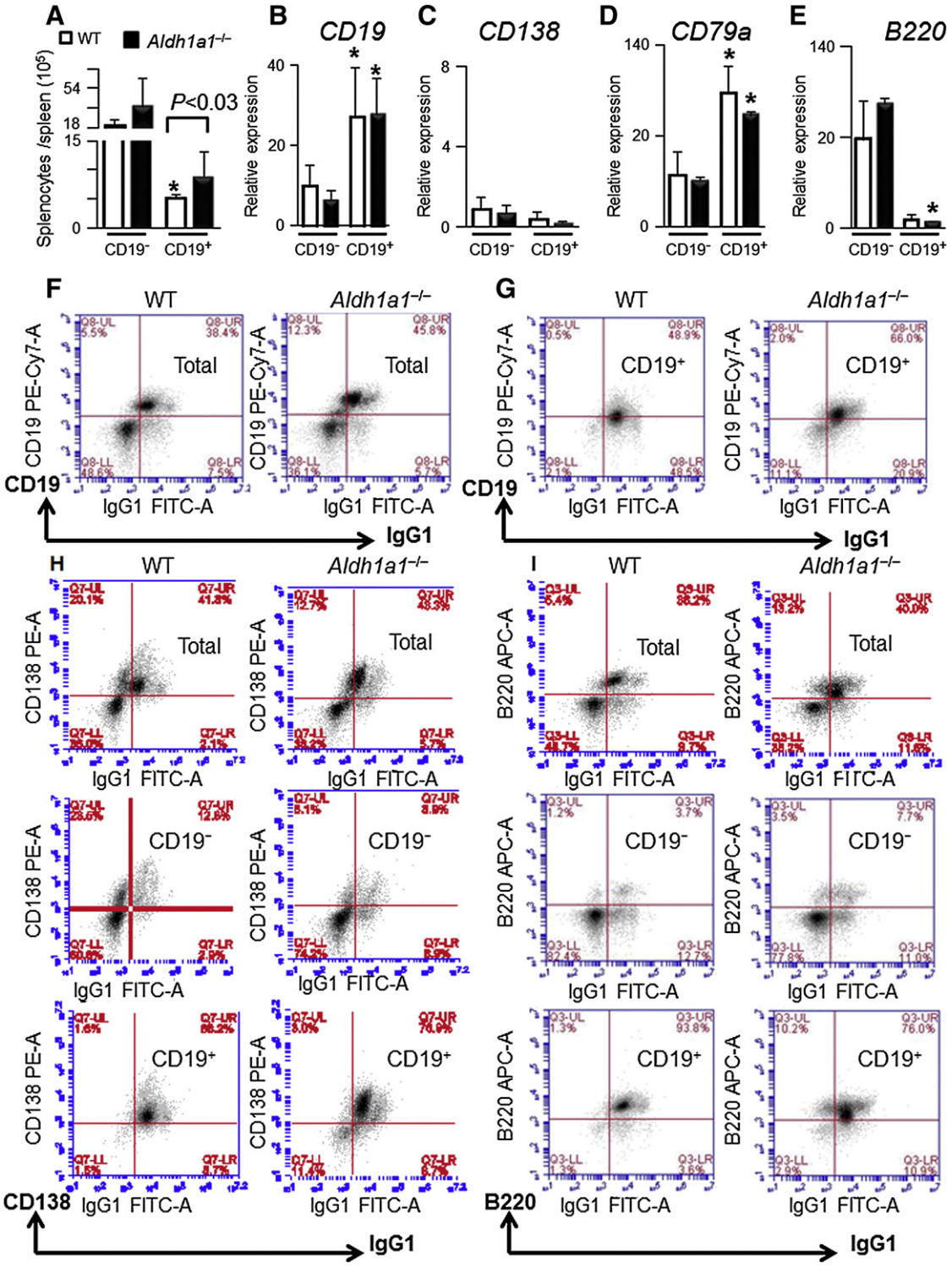

Fig. 2. Increased proportion of CD19$^+$B cells contributes to splenomegaly in *Aldh1a1*$^{-/-}$ mice. (A) CD19$^-$ and CD19$^+$ B cells were isolated from whole spleens of WT and *Aldh1a1*$^{-/-}$ mice using automated magnetic cell separation and double selection with IgG1 and CD19 antibodies (n = 5 per group). Cell populations were quantified. (B–E) Expression of CD19 (B) and plasma markers (CD138) (C) as well as differentiation (CD79a, D) and naive (B220, E) B cell markers were quantified in the isolated CD19$^-$ and CD19$^+$ B cells using TaqMan assays (n = 3 from each group). Data were normalized by *TBP*. Asterisk, significant difference in expression between CD19$^-$ and CD19$^+$ B cells of the same genetic background. Mann–Whitney *U* test. (F–I) Representative immunostaining characteristics (from n = 5 per group) of total splenocytes (F) and isolated CD19$^-$ and CD19$^+$ B cells (G) using FACS analysis. Total splenocytes and isolated CD19$^-$ and CD19$^+$ B cells were simultaneously analyzed with CD19, CD138 (H), and B220 (I) antibodies conjugated with different secondary fluorescent antibodies. For all gates, the percent and total count of all cells staining positive for both antibodies were determined.

transfected with human full length *Aldh1a1* (PCMV6-XL5, OriGene) or empty vector, using the Amaxa Cell Line Nucleofector Kit C (Lonza, NJ). Transient transfections were performed in NIH-3T3 fibroblasts lacking *Pparg* expression using Fugene (Roche, South San Francisco, CA) and the following vectors: HoxA10 luciferase reporter vector (Switchgear Genomics, Menlo Park, CA), control Renilla reporter vector, and murine full length *Rara*, *Pparg*, and *Rxra* constructs according to a previous protocol [16,20].

2.10. Statistical analysis

Oncomine cancer transcriptome database (https://www.oncomine.org) was used as a publicly available platform for data-mining in mRNA-expression studies [30]. The search terms '*Aldh1a1* and multiple myeloma' were used to identify relevant studies with sufficient sample numbers to compare expression of *Aldh1a1* in multiple myeloma and plasma cells in the same dataset. One such dataset was identified [31]. All other data group comparisons were performed using Mann Whitney *U*-test unless otherwise indicated, and correlations were examined by Pearson's test.

3. Results

3.1. Vitamin A metabolism regulates immature B cell populations in the spleen

The topography of RAR activation in mouse spleen was assessed in RARE-lacZ mice treated with and without RA (Fig. 1A). RARE activation in the spleen was heterogeneous and was predominant in the red pulp compared to lymphoid follicles in both non-treated and RA-treated samples.

RA is produced by an ALDH1 family of enzymes ALDH1a1, ALDH1a2, and ALDH1a3. In *Aldh1a1*$^{-/-}$ mice, the spleen is enlarged (256%, Fig. 1B) compared to spleens in WT mice. Spleen architecture is altered in *Aldh1a1*$^{-/-}$ vs. WT mice (Fig. 1C) due to the increased proportion of CD19$^+$ and B220$^+$ B cell populations (Fig. 1D). Germinal center markers MTA3 and BCL6 [32] were expressed at similar levels in *Aldh1a1*$^{-/-}$ and WT spleens, indicating that they were not impaired by *Aldh1a1* deficiency (Fig. 1E). The expression of *Cd1d1* was 61% lower in *Aldh1a1*$^{-/-}$ than in WT splenocytes. The association of splenomegaly with the increase in CD19$^+$ and B220$^+$ B cell populations suggests that differentiation could be impaired in *Aldh1a1*$^{-/-}$ mice.

Differentiated CD19$^+$ B cells are one of the major leukocyte populations in red pulp. Among them, the IgG1$^+$ B cell population was sensitive to RA in pharmacological studies [3,4]. Therefore, we used magnetic cell separation technology to separate IgG1$^+$/CD19$^-$ and IgG1$^+$/CD19$^+$ splenic B cell populations (Fig. 2) to test for effects of *Aldh1a1* deficiency on transcriptional regulation of critical immune pathways in B cells. We termed IgG1$^+$/CD19$^-$ as CD19$^-$ and IgG1$^+$/CD19$^+$ as CD19$^+$ B cells throughout the publication. The splenomegaly seen in *Aldh1a1*$^{-/-}$ mice (Fig. 1B) was associated with an increased number of CD19$^+$ B cells (171%) compared to WT (Fig. 2A). The purity and characteristics of CD19$^+$ B cell population were examined using *CD19* expression (Fig. 2B) and FACS analysis (Fig. 2F–G). Although both cell populations expressed similar low levels of plasma cell marker *CD138* (Fig. 2C), both CD19$^+$ and CD19$^-$ B cell populations were CD138-positive in FACS analysis (Fig. 2H). CD19$^+$ B cells also expressed a mature B cell marker CD79a (Fig. 2D). In contrast, an expression of pro-, mature and activated B cell marker B220 was lower in CD19$^+$ than in CD19$^-$ B cells (Fig. 2E). Both groups were B220 positive in FACS analysis (Fig. 2I). Notably, the expression of all major studied B cell markers was similar in WT and *Aldh1a1*$^{-/-}$ mice. However, *Aldh1a1* deficiency was associated with an increase in the CD19$^+$ B cell population and splenomegaly.

3.2. Dissimilar expression of Aldh1 in CD19$^-$ and CD19$^+$ B cell populations

To investigate whether CD19$^-$ and CD19$^+$ B cells metabolize vitamin A, we examined the expression of enzymes involved in synthesis of Rald (Fig. 3A) and RA (Fig. 3B). The expression of major Rald-generating enzymes (*Rdh10*, *Adh4*) was similar between CD19$^-$ and CD19$^+$ B cells (Fig. 3A, left panel). *Aldh1a1* deficiency moderately decreased *Rdh10* levels (−24%, Fig. 3A, right panel). In contrast, expression of the RA-generating *Aldh1a1* and *Aldh1a2* enzymes was markedly reduced to 6.4% and 18%, respectively, in CD19$^+$ compared to CD19$^-$ B cells (Fig. 3B left panel). *Aldh1a1* was the predominantly expressed member of ALDH1 family of enzymes in both CD19$^-$ and CD19$^+$ B cells (Fig. 3B, left panel). *Aldh1a1* deficiency suppressed the expression of *Aldh1a2* in CD19$^-$ and CD19$^+$ B cells (Fig. 3B, right panel). Thus, CD19$^+$ B cells in *Aldh1a1*$^{-/-}$ mice had reduced levels of all RA-producing enzymes. The change in *Aldh1a1* expression also influenced expression of *Rara*, the primary transcription factor regulated by RA [18]. *Rara* was reduced to 44% in CD19$^+$ vs. CD19$^-$ B cells in WT mice (Fig. 3C, left panel). In *Aldh1a1*$^{-/-}$ CD19$^-$ B cells, *Rara* expression was decreased to 60% compared to WT CD19$^-$ B cells and became similar to that seen in CD19$^+$ B cells (Fig. 3C, right panel).

3.3. Aldh1a1 deficiency results in oncogene expression in CD19$^+$ B cells

To identify the mechanisms altering the number and properties of CD19$^+$ B cells in *Aldh1a1*$^{-/-}$ mice, we analyzed the classic markers of

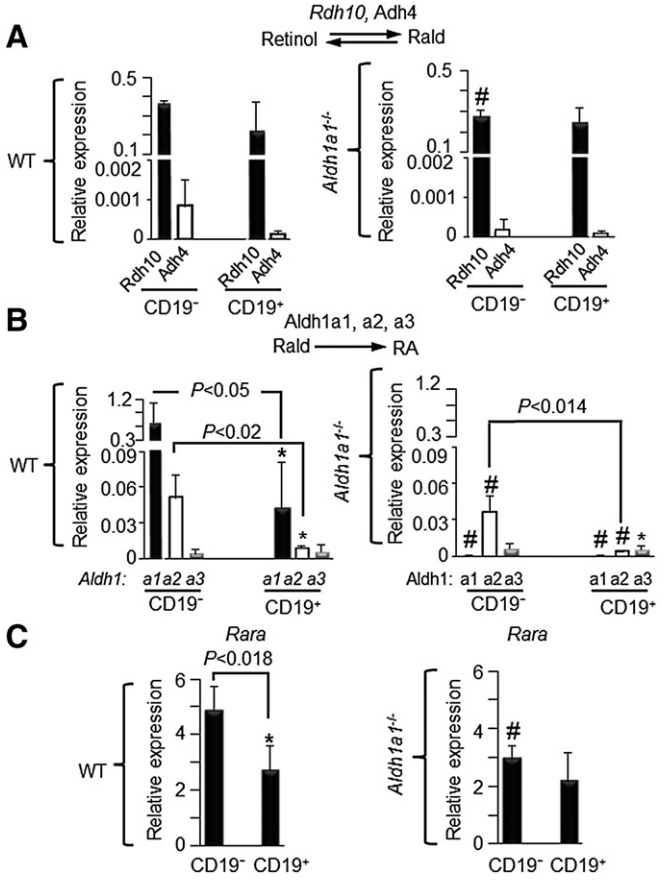

Fig. 3. Diminished expression of RA-generating *Aldh1* enzymes and *Rara* in B cells from *Aldh1a1*$^{-/-}$ vs. WT mice. (A–C) CD19$^-$ and CD19$^+$ B cells (same as in Fig. 2A, n = 5 per group) isolated from WT (left panels) and *Aldh1a1*$^{-/-}$ (right panels) mice were examined for the expression of (A) major retinaldehyde (Rald)-generating enzymes *Rdh10* and Adh4, (B) RA-generating enzymes *Aldh1a1*, *Aldh1a2*, and *Aldh1a3*, and (C) *Rara*. Gene expression was analyzed by TaqMan assays and normalized with *TBP*. *P*, significant difference in expression between CD19$^-$ and CD19$^+$ B cells. Mann–Whitney *U* test (throughout this figure).

B cell apoptosis (caspase 3), proliferation (Mki67) (Fig. 4A), and differentiation (Ebf1 and Pax 5) in all groups (Fig. 4B). The expression of these genes was not altered between *Aldh1a1*$^{-/-}$ vs. WT genotype in the isolated CD19^{-} and CD19^{+} B cells. *Ebf1* and *Pax5* expressions were higher in differentiated CD19^{+} than in CD19^{-} splenocytes; however, these levels were not influenced by WT and *Aldh1a1*$^{-/-}$ genotypes. To identify genes increasing CD19^{+} B cell population in *Aldh1a1*$^{-/-}$ mice, we quantified the expression of 250 inflammatory genes using NanoString Technologies' nCounter System. Gene expression was normalized using six housekeeping genes. The gene cluster analysis revealed that *Aldh1a1* influenced expression of proto-oncogenes (*c-Fos*, *c-Jun*, and *Mafk* kinase) and an opsonin (*C1qb*) (Fig. 4C). *Aldh1a1*$^{-/-}$ CD19^{-} B cells expressed 267% higher levels of *c-Fos* than WT cells (Fig. 3D). These changes were in agreement with decreased expression of *Rara*, a known suppressor of *c-Fos*, in CD19^{-} B cells (Fig. 3C) [33]. *Aldh1a1* deficiency affected CD19^{+} B cells more than CD19^{-} B cells. Specifically *c-Fos* and *c-Jun* expression levels were 711% and 294% higher than those in WT cells (Fig. 4D). This finding was paradoxical because CD19^{-} B cells expressed 15.5-times higher *Aldh1a1* and 5.5-times higher *Aldh1a2* levels than those seen in CD19^{+} B cells from WT mice (Fig. 3B). We hypothesized that another *Aldh1a1*-sensitive suppressor of *c-Fos*/*c-Jun* is active in CD19^{+} B cells.

3.4. Aldh1a1 limits oncogene expression CD19^{+} B cells by a sequential induction of Zfp423 and Pparg

ALDH1 enzymes can induce the transcription factor *Zfp423* which, in turn, controls the expression of the anti-proliferative and anti-inflammatory transcription factor *Pparg* in adipocytes [20]. In splenic B cells, expression of *Aldh1a1* positively correlated with *Zfp423*, specifically in CD19^{+} B cells ($P < 0.001$) (Fig. 5A). *Zfp423* was markedly up-regulated in CD19^{+} (625%) vs. CD19^{-} WT B cells. However, this increase was abolished in *Aldh1a1*$^{-/-}$ CD19^{+} B cells (Fig. 5B), suggesting a regulatory role of *Aldh1a1*. The *Zfp423* expression levels were also

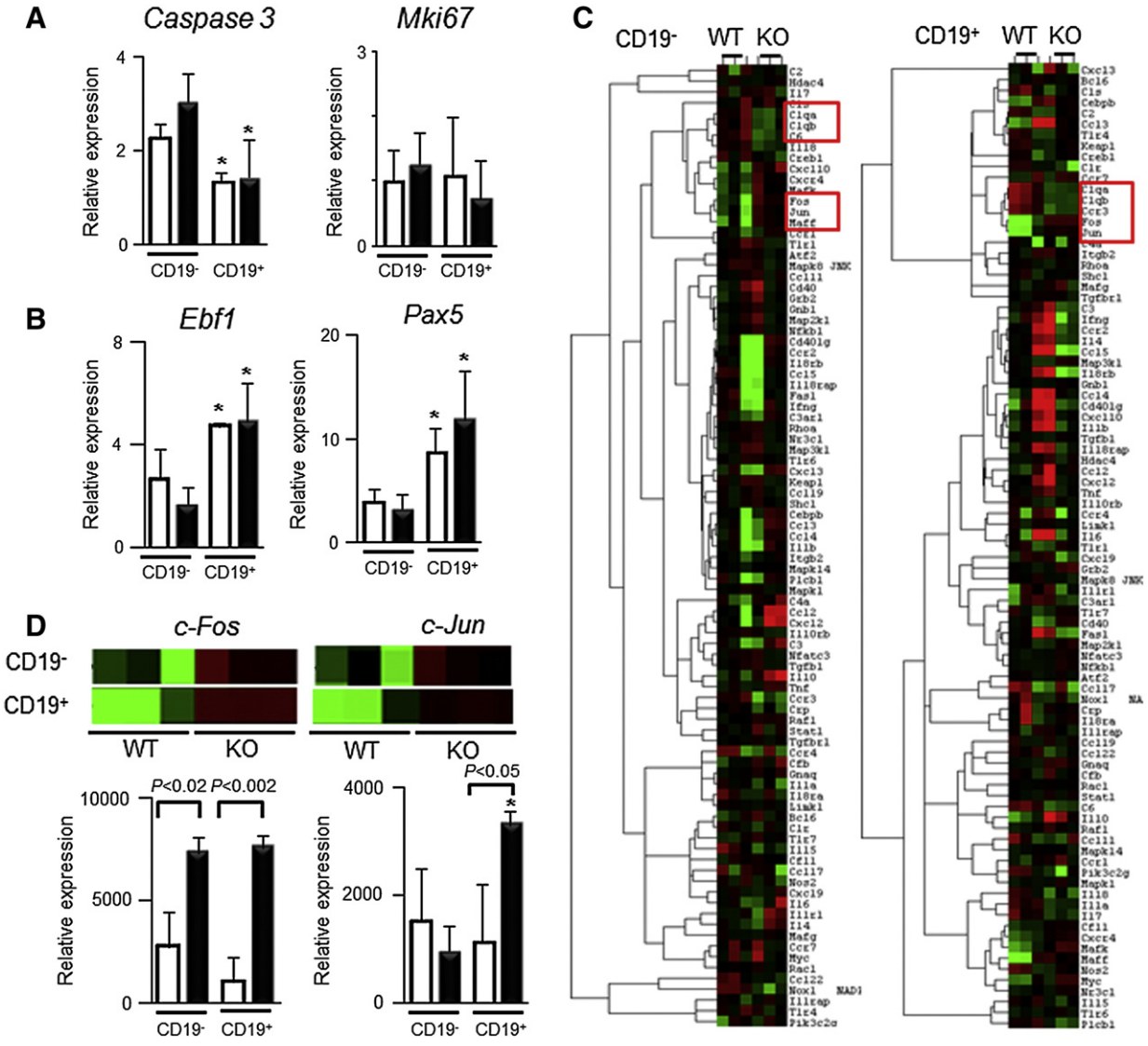

Fig. 4. Increased expression of proto-oncogenic genes in isolated splenic CD19^{-} and CD19^{+} *Aldh1a1*$^{-/-}$ vs. WT B cells. CD19^{-} and CD19^{+} B cells were isolated from spleens of the same WT (white bars) and *Aldh1a1*$^{-/-}$ (black bars) group of mice (Fig. 2, n = 5 per group). (A & B) Expression of apoptosis (caspase3) and proliferation markers (Mki67) (A) as well as B cell differentiation markers (*Ebf1* and *Pax5*) were semi-quantified using TaqMan assays. Data (n = 3 per group) were normalized by *TBP*. Asterisk, significant difference in expression between CD19^{-} and CD19^{+} B cells of the same genetic background. Mann–Whitney *U* test. (C) Selected expression heat maps (red and green colors represent high and low expression levels, respectively) obtained using NanoString Technologies' nCounter mouse inflammation panel. The nCounter GX Mouse Inflammation Kit (NanoString Technologies) consists of 184 inflammation-related genes and six internal reference genes (www.nanostring.com). Red boxes showed statistically significant (n = 3 per group, $P < 0.05$, Mann–Whitney *U* test) clusters of genes. (D) Expression levels of *c-Fos* and *c-Jun*, using NanoString Technologies' nCounter mouse inflammation panel insets show the extracted expression heat maps for *c-Fos* and *c-Jun*. *P*, significant difference between WT and *Aldh1a1*$^{-/-}$ B cells, Mann–Whitney *U* test (n = 3 per group).

correlated with *Pparg* levels in CD19$^+$ B cells (Fig. 5C). In agreement with *Zfp423*'s role in the induction of *Pparg* [20], only CD19$^+$ B cells expressed less *Pparg* (−75%) in *Aldh1a1*$^{-/-}$ than WT splenocytes (Fig. 5D). PPAR response element (PPRE) has been identified in the promoter of transcription factor *Hoxa10* [34], a key inducer of human lymphomyelopoiesis [35]. To examine a possible role for *Pparg* in the regulation of the *Hoxa10* promoter, we performed transfection studies in NIH 3T3 fibroblasts, a cell line lacking endogenous *Pparg* expression. Forced expression of *Pparg* inhibited activation of *Hoxa10* promoter in a gene dose-dependent manner (Fig. 5E). *Pparg* expression also markedly suppressed *Hoxa10* promoter activation in a ligand (rosiglitazone)-dependent manner (Fig. 5F). In contrast, both *Rxra* and *Rara* only moderately activated *Hoxa10* promoter reporter in the presence or absence of RA ligand (Fig. 5G). Consistent with a regulatory role of *Pparg*, CD19$^+$ B cells expressed 400% higher levels of *Hoxa10* in *Aldh1a1*$^{-/-}$ than in WT mice (Fig. 5H). Thus, elevated *Hoxa10* expression in *Aldh1a1*$^{-/-}$ CD19$^+$ B cells could be a direct effect of deficient *Pparg* expression. Other transcriptional mechanisms may also regulate *Hoxa10* in CD19$^-$ B cells. Since elevated expression of proto-oncogenes AP1 (*c-fos*/*c-jun*) and *Hoxa10* is involved in the development of multiple myeloma (MM), we examined the *Aldh1a1* expression in B-cell related cancers.

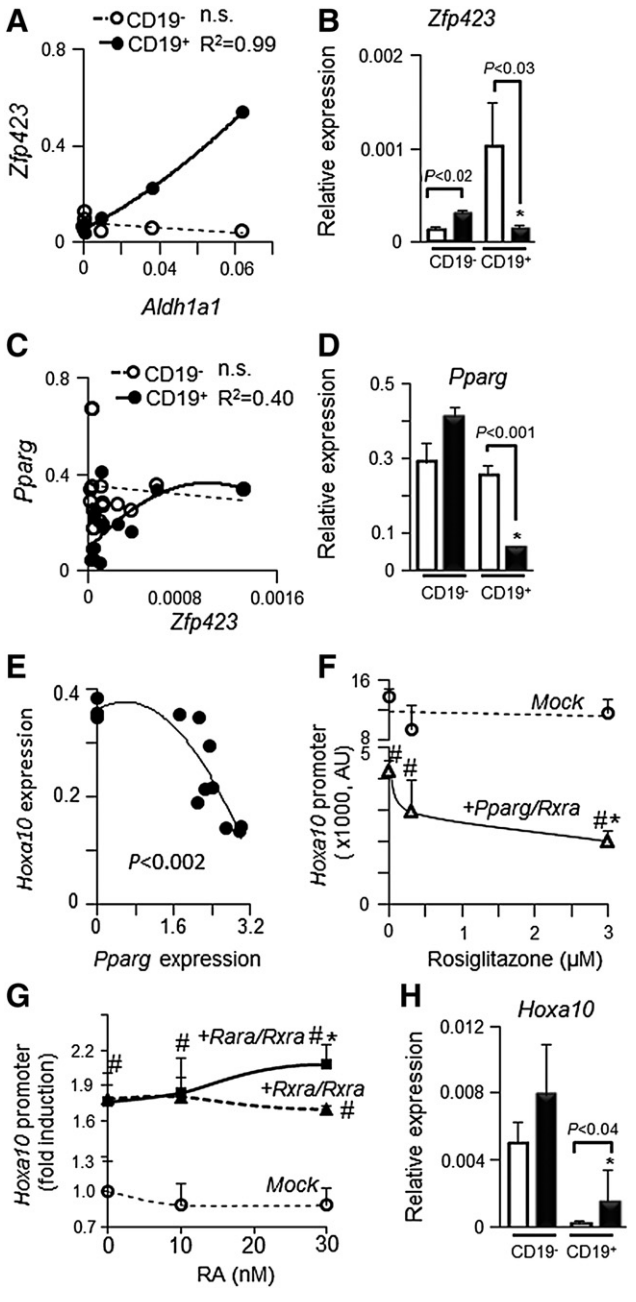

3.5. RA and/or Aldh1a1 rescues Rara and Zfp423 expressions in myeloma B cell lines

A search of publicly-available cancer gene expression data using Oncomine analysis revealed that B-cell-related cancer cell lines express low levels of *Aldh1a1* compared to other cancer cell lines (Fig. 6A). In our studies in peripheral blood mononuclear cells isolated from healthy donors (Fig. 6B), *Aldh1a1* was a predominantly expressed gene from the ALDH1 family. This pattern of expression was markedly changed in MM cell lines U266B1, RPMI8266, OPM2, L363, and MM1s (Fig. 6B). L363 MM cells expressed no *Aldh1* genes. *Aldh1a1* expression was lower compared to the expression of *Aldh1a2* and *Aldh1a3* in these MM cells. In agreement, the Oncomine analysis findings [31] showed reduced *Aldh1a1* expression in 74 human MM patients, compared to healthy plasma cell controls (Fig. 6C). The RA stimulation of L363 MM cells increased expression of *Znf423*, a human analog of murine *Zfp423* in MM cells (Fig. 6D). *Aldh1a1* overexpression was even more effective in up-regulating suppressors of proto-oncogenes. The expression of a full-length human *Aldh1a1* construct increased *Aldh1a1* expression in U266 MM cells without altering expression of *Aldh1a2* and *Aldh1a3* (Fig. 6E). This overexpression of *Aldh1a1* resulted in an increased expression of both *Rara* (30%) and *Znf423* (500%) in U266 MM cells (Fig. 6F).

4. Discussion

Humoral immune responses are mediated by mature follicular B cells with the help of T cells in splenic germinal centers and, to a minor extent (~10%), by marginal-zone B cells [2]. Cytokines/cytokine receptors, Ig recognition, and antigen presented by APCs, dendritic cells, and/or macrophages can initiate differentiation of B cells and formation of germinal centers to achieve Ig production [11]. In these processes, dietary vitamin A or RA can facilitate differentiation by classic Pax5-dependent pathways in some splenic B cell population [11,12]. Our study revealed a key role for RA-generating ALDH1 enzymes in B cell biology. *Aldh1a1* expression in immature CD19$^+$ B cells and MM B cells is critical for the establishment of a transcriptional profile (Fig.7) that prevents oncogene expression.

Fig. 5. *Aldh1a1* influences expression of *Zfp423* and *Pparg* genes in CD19$^+$ B cells, suppressing promoter activity of *Hoxa10*. (A & B) Correlation (A) between *Aldh1a1* expression (Aldh1a1 expression was shown in Fig. 3B) and expression levels of *Zfp423* (B) in CD19$^-$ (white bars or circles) and CD19$^+$ (black bars or circles) B cells. Gene expression was analyzed in triplicate by TaqMan assays (n = 3 per group). (C & D) Correlation (C) between *Zfp423* expression (B) and expression levels of *Pparg* (D) in CD19$^-$ (white bars or circles) and CD19$^+$ (black bars or circles) B cells (n = 6 in each correlation group). Gene expression was analyzed by TaqMan assays in triplicate. Asterisk, significant difference in expression between CD19$^-$ and CD19$^+$ B cells of the same genetic background; *P*, significant difference between WT and *Aldh1a1*$^{-/-}$ B cells, Mann–Whitney *U* test. (E–G) Promoter analysis of *Hoxa10* in NIH3-3T3 fibroblasts lacking *Pparg* (n = 12). (E) NIH3-3T3 fibroblasts were transiently transfected with full-length *Pparg* overexpression or empty (mock) vector (0). 48 h after transfection the expression of *Hoxa10* was measured by TaqMan assay. *P*, Pearson correlation. (F) Promoter analysis of *Hoxa10* in NIH3-3T3 fibroblasts transiently transfected with mock or full-length *Pparg* overexpression vectors. 24 h after transfection, cells were stimulated with different rosiglitazone concentrations for 15 h (n = 3 in each stimulated group). #, significantly different between cells expressing mock and *Pparg* vector; asterisk, significant difference between *Pparg* expressing cells stimulated with vehicle and rosiglitazone. (G) Cell was transiently transfected with empty vector (Mock) or *Rara* and *Rxra* overexpression vectors (n = 9). 24 h after transfection, cells were stimulated with different retinoic acid (RA, n = 3) concentrations for 27 h. #, significantly different between cells expressing empty vector and *Rara* and/or *Rxra*; asterisk, significant difference between *Rara*/*Rxra* expressing cell stimulated with vehicle (ethanol/DMSO, 50/50%) and RA, Mann–Whitney *U* test. (H) Expression levels of *Hoxa10* in CD19$^-$ (white bars or circles) and CD19$^+$ (black bars or circles) B cells measured by TaqMan assay (n = 3 for each group). Significance was determined as in (D).

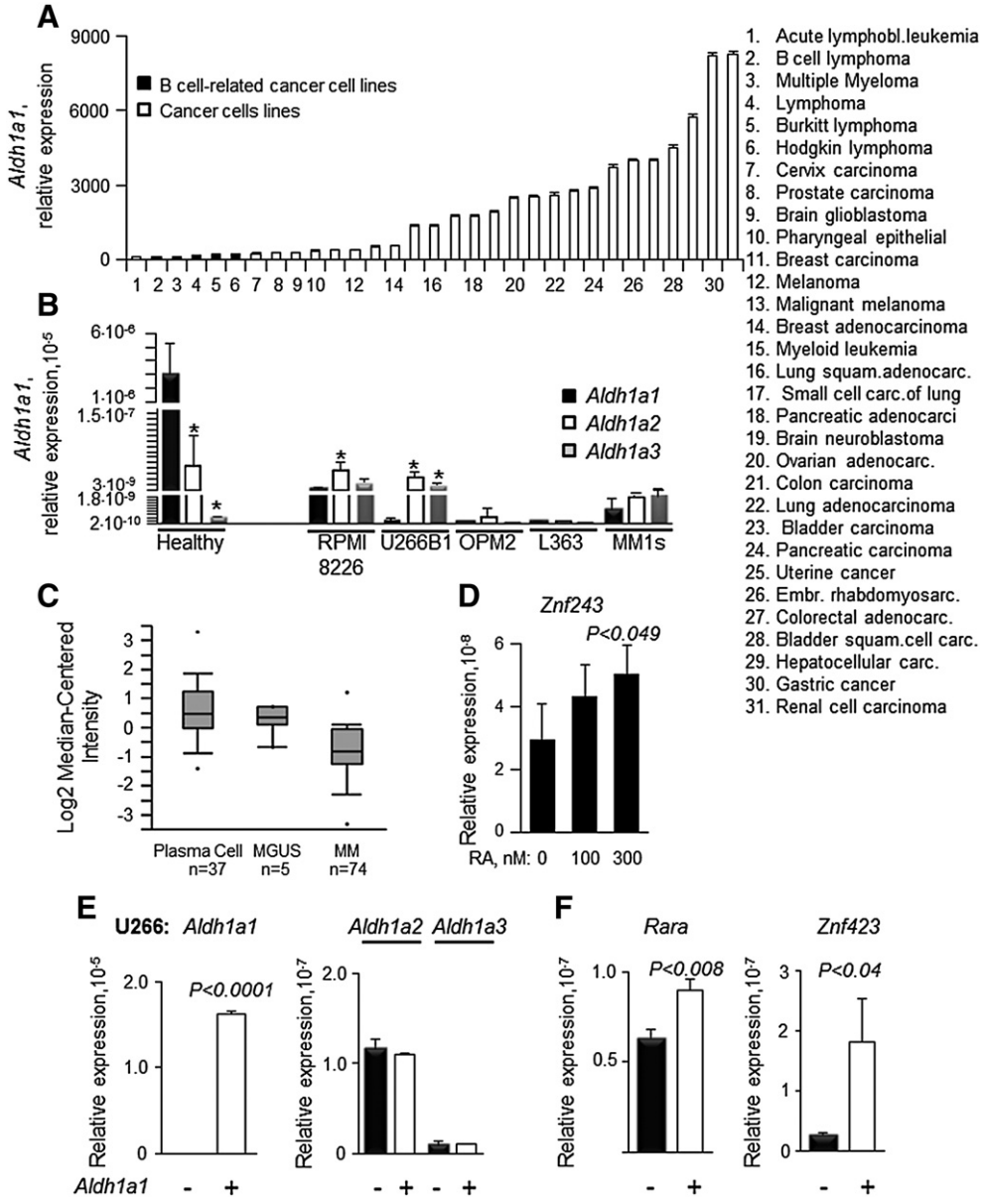

Fig. 6. Impaired *Aldh1a1* expression in human multiple myeloma B cell lines could be rescued by RA or Aldh1a1 overexpression that increased *Rara* and *Znf423* levels. (A) Relative expression of Aldh1a1 in hematological (n = 3) and other cancer cell lines (n = 28). Data were obtained from data mining in Oncomine database and based on the publication by Rhodes et al. [30]. (B) Expression levels of *Aldh1* genes were measured in human PBMC cells (n = 7 donors) and in myeloma cell lines (n = 5): RPMI, U266B1, OPM2, L363, and MM1s (n = 3 per measurement). *P*, significant difference in expression between *Aldh1a1*, *Aldh1a2*, and *Aldh1a3* enzymes within the same cell population. (C) Analysis of *Aldh1a1* gene expression in human multiple myeloma (n = 74), plasma cells (n = 37) and monoclonal gammopathy of undetermined significance (MGUS) (n = 5). Gene expression database analysis (see Materials and methods) identified by Zhan et al. (2002) [31] data shown here (adapted from Oncomine; Rhodes et al. (2007) [30]). The plot boxes are lined at lower, median and upper quartile score values; whiskers extend to 10th and 90th percentiles; dots mark minimum and maximum values. (D) RA treatment of L363 myeloma cell lines increases *Znf*423 expression. L363 cells were maintained in RPMI medium containing 1% of UV treated FBS, which is depleted of retinoids. L363 cells were maintained in this medium 24 h prior to RA stimulation and during treatment with RA. *Znf243* expression was measured 48 h after RA treatment (n = 3). *P*, significant difference, Mann–Whitney *U* test. (E) Expression levels of *Aldh1a1* (left panel) and *Aldh1a2* and *Aldh1a3* (black and white bars in the right panel) in U266B1 cells transiently transfected with empty (−) or human full length Aldh1a1 overexpression plasmid (+) (n = 3 independent experiments). Expression levels were measured in triplicate using TaqMan assays 24 h after transfection. *P*, significant difference, Mann–Whitney *U* test. (F) Expression of *Rara* (left panel) and *Znf*423 (human analog of mouse*Zfp423*, right panel) in U266B1 (black bar) transfected with empty (−) and *Aldh1a1* overexpression vector (+) (n = 3 independent experiments). *P*, significant difference, Mann–Whitney *U* test.

Aldh1a1 expression was consistently predominant over other RA-generating enzymes from the ALDH1 family in healthy B cells in mice and humans (Figs. 3B and 6B). *Aldh1a1*-dependent pathways in isolated B cell populations were different from those altered by administration of RA or manipulation of dietary vitamin A content. RA administration has two major sites of action related to B cell functions. It improves antigen presentation and IgA production at mucosal sites [15] and induces proliferation and differentiation of $IgG1^+$ splenocytes in germinal centers [3,4,11]. In these scenarios, endogenous RA was produced by APCs and stimulated final B cell differentiation in germinal centers [36]. We showed that under physiological conditions, intense endogenous RAR activity was associated with red pulp (Fig. 1A). In agreement, we found the highest *Aldh1a1* and *Rara* expression levels in $IgG1^+CD19^-$ ($CD19^-$) B cell populations (Figs. 2, 3). $CD19^-$ is a potentially heterogeneous population comprised of naive and mature $B220^+$ B cell populations. Both *Rara* and *Aldh1* expressions were decreased in the $IgG1^+CD19^+$ ($CD19^+$) population. This loss of endogenous RA production in $CD19^+$ B cells could later allow them to receive a paracrine signaling of RA-producing APCs after they enter germinal centers. The physiological expression of *Aldh1* genes in $CD19^+$ vs. $CD19^-$ B cells in WT mice

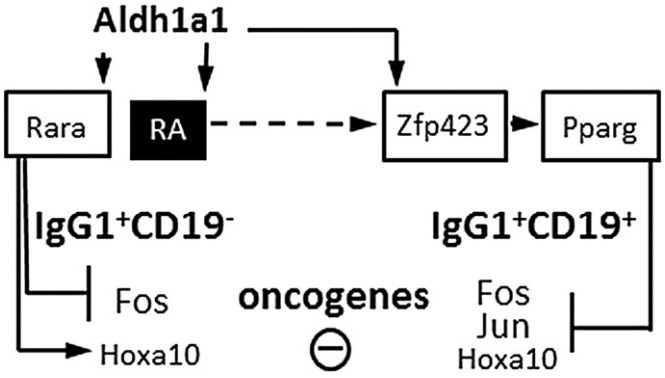

Fig. 7. Schematic diagram of the *Aldh1a1* dependent pathways in CD19$^-$ and CD19$^+$ IgG1$^+$ B cell populations in the spleen. *Aldh1a1* is expressed at higher levels in CD19$^-$ vs. CD19$^+$ B cells. *Aldh1a1* also shapes the expression of transcription factors in CD19$^+$ population, where it is responsible for the induction of *Zfp423* and *Pparg*. Expression of *Pparg* suppressed proto-oncogenes *c-Fos*, *c-Jun*, and *Hoxa10*.

prevented increase in expression of oncogenes *c-Fos*/*c-Jun* and *Hoxa10* (Figs. 4D, 5H), due to the *Aldh1a1*-dependent induction of oncogene suppressors (*Zfp423 and Pparg*) in these cells (Fig. 5B, D). The disruption of *Aldh1a1* regulation in *Aldh1a1*$^{-/-}$ mice markedly compromised B cell oncogene profiles during differentiation (Figs. 4, 5), increased red pulp proportions, and reduced expression of *Cd1d1* that is involved in interactions between T and B cells (Fig. 1D, right panel).

Classic CD19$^-$ and CD19$^+$ B cell differentiation via *Ebf1* and *Pax5* [37] appear to be not impaired in the absence of *Aldh1a1* (Fig. 4B). The breakthrough in the understanding of the mechanism increasing CD19$^+$ population came from the NanoString analysis (Fig. 4C). *Aldh1a1* deficient CD19$^+$ B cells expressed proto-oncogenes *c-Fos*/*c-Jun* forming the transcription factor AP1. Elevated *c-Fos*/*c-Jun* and also *Hoxa10* expressions are distinct features of B cell-dependent hematological neoplasms, including lymphomas and multiple myeloma [38–40]. *Hoxa10* overexpression in hematopoietic cells is sufficient to impair murine and human lymphomyelopoiesis and leads to acute myeloid leukemia [35,41]. Notably, all five human multiple myeloma (MM) cell lines expressed 100-times less *Aldh1a1* than normal PBMC cells (Fig. 6B). Similar findings in B cell cancers and in plasma cells from MM patients were available from other studies [31] that we identified through database analysis (Fig. 6A, C). The major RA-generating enzyme in these cancer cells was *Aldh1a2* suggesting that the loss of *Aldh1a1* contributed to B cell neoplastic pathology. Previous studies showed that only combined treatment of RA and rosiglitazone can induce U266 differentiation [14]. Our data provide a mechanism and rationale for the treatment of MM B cells lacking *Aldh1a1* with RAR and PPARγ agonists.

Increased *c-Fos* expression in *Aldh1a1*$^{-/-}$ CD19$^-$ B cells appears to be consistent with the known competitive relation between AP1 and RARα activated by RA [33]. Indeed, *Aldh1a1*$^{-/-}$ CD19$^-$ B cells had reduced expression of both *Aldh1a1* and *Rara* (Fig. 3). Forced expression of *Aldh1a1* in U266 cells can readily increase *Rara* expression (Fig. 6). An unexpected result of our study was the finding of more profound transcriptional changes in CD19$^+$ compared to CD19$^-$ B cells expressing markedly less *Aldh1a1* in WT mice (Fig. 3B). WTCD19$^+$ cells expressed higher levels of proto-oncogenes *c-Fos*, *c-Jun*, and *Hoxa10* than *Aldh1a1*$^{-/-}$ CD19$^+$ B cells. Increased number of CD19$^+$ cells contributed partially to the splenomegaly in *Aldh1a1*$^{-/-}$ mice. This phenomenon could be based on *Aldh1a1*-mediated changes on the transcriptome. During adipogenesis, *Aldh1a1* induces expression of the transcription factor *Zfp423*, which in turn induces *Pparg* [20,42]. Previous investigations highlighted competition between *Pparg* and *c-Fos*/*c-Jun* without engaging PPRE [43,44]. PPRE response element was found in the *Hoxa10* promoter [34]. Our studies connected *Aldh1a1* to the regulation of all these transcription factors in B cells (Fig.7). *Aldh1a1* did not support *Zfp423* expression in CD19$^-$ B cells probably due to the specific transcriptional environment. It is possible that high *Aldh1a1* levels in CD19$^-$ B cells produced RA for paracrine signaling that induced *Zfp423* in CD19$^+$ B cells. These regulatory mechanisms remain to be investigated in the future. We found that *Aldh1a1* is required for the *Zfp423* induction in differentiating CD19$^+$ population (Fig. 5B). *Zfp423* and *Pparg* levels were higher in CD19$^+$ B cells in WT compared to *Aldh1a1*$^{-/-}$ mice. This link was suggested by a significant correlation in CD19$^+$ B cells (Fig. 5C). The causative link between *Aldh1a1* and *Zfp423* expressions was demonstrated in human U266 MM cells. *Aldh1a1* expression rescued *Znf423* (human analog of mouse *Zfp423*) in U266 MM cells (Fig. 6F). RA treatment of MM cells can also rescue *Znf423* expression (Fig. 6D), suggesting that ALDH1a1 acts in part via autocrine RA generation. Since *Pparg* is induced by *Znf423*, the short (24 h) transfection period was not sufficient to also observe significant increase in *Pparg* expression. However, the relationship between *Zfp423* and *Pparg* has been widely documented [20,42]. *Pparg* induction by *Aldh1a1* appears to be a critical event, because *Pparg* was an effective suppressor of *Hoxa10*, a key transcription factor perturbing myeloid and lymphoid differentiation in mice and humans [34,35,41]. *Pparg* inhibited the promoter of *Hoxa10*, while *Rara* and *Rxra* only modestly regulated this transcription factor (Fig. 5F, G). Consequently, *Hoxa10* was upregulated in *Aldh1a1*$^{-/-}$ CD19$^+$ B cells expressing less *Pparg*. Studies investigating the effects of vitamin A-deficient diets reported splenomegaly and an increase in plasma IgG1 levels in mouse models of autoimmune disorders [45], whereas the production of specific IgG1 antibodies in the immunized mice was impaired [46]. Multiple mechanisms have been proposed to explain these phenomena, including RA-dependent production of IFNγ from T cells [47] and dendritic CD103$^+$ cell subsets [48], but the role of B cells was unclear. Our data highlight an autocrine and/or paracrine ALDH1 function in differentiating B cells that regulates two key transcriptional oncogene suppressors *Rara* and *Pparg*. This suggests a gene–environment paradigm for early-stage deregulation of oncogene profiles in IgG1$^+$ B cell subsets through compromised vitamin A metabolism.

5. Conclusion

Our findings showed the critical role of the retinoic acid-generating ALDH1a1 enzyme in the sequential induction of oncogene suppressors *Rara* in IgG1$^+$/CD19$^-$ B cells and *Zfp423*/*Pparg* in IgG1$^+$/CD19$^+$ B cells during B cell differentiation. In the absence of these suppressors, B cells acquire oncogene *Ap1* and *Hoxa10* expressions that lead to IgG1$^+$/CD19$^+$ B cell expansion and splenomegaly. Reduced expression of *Aldh1a1* and oncogene suppressors *Rara*, *Zfp423*, and *Pparg* is a characteristic property of malignant human multiple myeloma B cells. Importantly, ectopic expression of *Aldh1a1* or RA effectively rescues *Rara* and/or *Zfp423* expression. The understanding of the role of ALDH1a1 in B cell differentiation can shed light on the early stages in the development of malignant hematological disorders and may lead to the development of novel therapeutics.

Funding

This research was supported by Food Innovation Center, Office for International Affairs and Center for Advanced Functional Foods Research and Entrepreneurship at OSU, Daskal Foundation (O.Z., R.Y.) and Multiple Myeloma Opportunities for Research and Education (MMORE, D.M.B.Jr). The project described was supported by award number grant UL1TR000090 from the National Center For Advancing Translational Sciences and the Cancer Center Support Grant (CA016058) (O.Z). This study was also supported in part by a research grant (CA100865) from the Department of Defense Congressionally Directed Medical Research Programs (C.E.A.). The content is solely the

responsibility of the authors and does not necessarily represent the official views of the National Center for Research Resources or the National Institutes of Health.

Acknowledgements

We thank Dr. C. Ross (Pennsylvania State University) for the helpful discussion. We express our gratitude to Kirsteen Maclean (NanoString Technologies) and the Nucleic Acid Shared Resource at The Ohio State University (OSU) for excellent technical and intellectual support.

References

[1] D.K. Dunn-Walters, A.A. Ademokun, B cell repertoire and ageing, Curr. Opin. Immunol. 22 (2010) 514–520.
[2] P. Matthias, A.G. Rolink, Transcriptional networks in developing and mature B cells, Nat. Rev. Immunol. 5 (2005) 497–508.
[3] Q. Chen, A.C. Ross, Inaugural article: vitamin A and immune function: retinoic acid modulates population dynamics in antigen receptor and CD38-stimulated splenic B cells, Proc. Natl. Acad. Sci. U. S. A. 102 (2005) 14142–14149.
[4] Q. Chen, A.C. Ross, Retinoic acid promotes mouse splenic B cell surface IgG expression and maturation stimulated by CD40 and IL-4, Cell. Immunol. 249 (2007) 37–45.
[5] J.M. Phillips-Quagliata, A.M. Faria, J. Han, D.H. Spencer, G. Haughton, P. Casali, IgG2a and IgA co-expression by the natural autoantibody-producing murine B lymphoma T560, Autoimmunity 33 (2001) 181–197.
[6] C.H. Kim, Roles of retinoic acid in induction of immunity and immune tolerance, Endocr. Metab. Immune Disord. Drug Targets 8 (2008) 289–294.
[7] A. Amouzou, O. Habi, K. Bensaid, Reduction in child mortality in Niger: a countdown to 2015 country case study, Lancet 380 (2012) 1169–1178.
[8] MMWR Morb. Mortal. Wkly. Rep. 56 (2007) 1237–1241.
[9] G.D. Hussey, M. Klein, A randomized, controlled trial of vitamin A in children with severe measles, N. Engl. J. Med. 323 (1990) 160–164.
[10] A. Ertesvag, S. Naderi, H.K. Blomhoff, Regulation of B cell proliferation and differentiation by retinoic acid, Semin. Immunol. 21 (2009) 36–41.
[11] A.C. Ross, Q. Chen, Y. Ma, Vitamin A and retinoic acid in the regulation of B-cell development and antibody production, Vitam. Horm. 86 (2011) 103–126.
[12] X. Chen, B.L. Esplin, K.P. Garrett, R.S. Welner, C.F. Webb, P.W. Kincade, Retinoids accelerate B lineage lymphoid differentiation, J. Immunol. 180 (2008) 138–145.
[13] D. Donjerkovic, C.M. Mueller, D.W. Scott, Steroid- and retinoid-mediated growth arrest and apoptosis in WEHI-231 cells: role of NF-kappaB, c-Myc and CKI p27(Kip1), Eur. J. Immunol. 30 (2000) 1154–1161.
[14] H. Huang, D. Wu, J. Fu, G. Chen, W. Chang, H.C. Chow, A.Y. Leung, R. Liang, All-trans retinoic acid can intensify the growth inhibition and differentiation induction effect of rosiglitazone on multiple myeloma cells, Eur. J. Haematol. 83 (2009) 191–202.
[15] M.J. Jorgensen, A.B. Fisker, E. Sartono, A. Andersen, C. Erikstrup, I.M. Lisse, M. Yazdanbakhsh, P. Aaby, C.S. Benn, The effect of at-birth vitamin A supplementation on differential leucocyte counts and in vitro cytokine production: an immunological study nested within a randomised trial in Guinea–Bissau, Br. J. Nutr. (2012) 1–11.
[16] R. Yasmeen, S.M. Jeyakumar, B. Reichert, F. Yang, O. Ziouzenkova, The contribution of vitamin A to autocrine regulation of fat depots, Biochim. Biophys. Acta 1821 (2012) 190–197.
[17] G. Duester, Retinoic acid synthesis and signaling during early organogenesis, Cell 134 (2008) 921–931.
[18] P. Germain, P. Chambon, G. Eichele, R.M. Evans, M.A. Lazar, M. Leid, A.R. De Lera, R. Lotan, D.J. Mangelsdorf, H. Gronemeyer, International Union of Pharmacology. LX. Retinoic acid receptors, Pharmacol. Rev. 58 (2006) 712–725.
[19] O. Ziouzenkova, Vitamin A metabolism: challenges and perspectives, Vitam. Miner. Elem. 1 (2012) E106.
[20] B. Reichert, R. Yasmeen, S.M. Jeyakumar, F. Yang, T. Thomou, et al., Concerted action of aldehyde dehydrogenases influences depot-specific fat formation, Mol. Endocrinol. 25 (2011) 799–809.
[21] D.M. Duriancik, K.A. Hoag, Vitamin A deficiency alters splenic dendritic cell subsets and increases CD8(+)Gr-1(+) memory T lymphocytes in C57BL/6J mice, Cell. Immunol. 265 (2010) 156–163.
[22] J.R. Mora, M. Iwata, B. Eksteen, S.Y. Song, T. Junt, et al., Generation of gut-homing IgA-secreting B cells by intestinal dendritic cells, Science 314 (2006) 1157–1160.
[23] J. Rossant, R. Zirngibl, D. Cado, M. Shago, V. Giguere, Expression of a retinoic acid response element-hsplacZ transgene defines specific domains of transcriptional activity during mouse embryogenesis, Genes Dev. 5 (1991) 1333–1344.
[24] X. Fan, A. Molotkov, S. Manabe, C.M. Donmoyer, L. Deltour, M.H. Foglio, A.E. Cuenca, W.S. Blaner, S.A. Lipton, G. Duester, Targeted disruption of Aldh1a1 (Raldh1) provides evidence for a complex mechanism of retinoic acid synthesis in the developing retina, Mol. Cell. Biol. 23 (2003) 4637–4648.
[25] R. Yasmeen, B. Reichert, J. Deiuliis, F. Yang, A. Lynch, et al., Autocrine function of aldehyde dehydrogenase 1 as a determinant of diet- and sex-specific differences in visceral adiposity, Diabetes 62 (2013) 124–136.
[26] O. Ziouzenkova, G. Orasanu, M. Sharlach, T.E. Akiyama, J.P. Berger, et al., Retinaldehyde represses adipogenesis and diet-induced obesity, Nat. Med. 13 (2007) 695–702.
[27] M. Sherger, W. Kisseberth, C. London, S. Olivo-Marston, T.L. Papenfuss, Identification of myeloid derived suppressor cells in the peripheral blood of tumor bearing dogs, BMC Vet. Res. 8 (2012) 209.
[28] G.K. Geiss, R.E. Bumgarner, B. Birditt, T. Dahl, N. Dowidar, et al., Direct multiplexed measurement of gene expression with color-coded probe pairs, Nat. Biotechnol. 26 (2008) 317–325.
[29] Y. Dai, T.H. Landowski, S.T. Rosen, P. Dent, S. Grant, Combined treatment with the checkpoint abrogator UCN-01 and MEK1/2 inhibitors potently induces apoptosis in drug-sensitive and -resistant myeloma cells through an IL-6-independent mechanism, Blood 100 (2002) 3333–3343.
[30] D.R. Rhodes, S. Kalyana-Sundaram, S.A. Tomlins, V. Mahavisno, N. Kasper, R. Varambally, T.R. Barrette, D. Ghosh, S. Varambally, A.M. Chinnaiyan, Molecular concepts analysis links tumors, pathways, mechanisms, and drugs, Neoplasia 9 (2007) 443–454.
[31] F. Zhan, J. Hardin, B. Kordsmeier, K. Bumm, M. Zheng, et al., Global gene expression profiling of multiple myeloma, monoclonal gammopathy of undetermined significance, and normal bone marrow plasma cells, Blood 99 (2002) 1745–1757.
[32] T. Okada, S. Moriyama, M. Kitano, Differentiation of germinal center B cells and follicular helper T cells as viewed by tracking Bcl6 expression dynamics, Immunol. Rev. 247 (2012) 120–132.
[33] X.F. Zhou, X.Q. Shen, L. Shemshedini, Ligand-activated retinoic acid receptor inhibits AP-1 transactivation by disrupting c-Jun/c-Fos dimerization, Mol. Endocrinol. 13 (1999) 276–285.
[34] Y. Gosiengfiao, R. Horvat, A. Thompson, Transcription factors GATA-1 and Fli-1 regulate human HOXA10 expression in megakaryocytic cells, DNA Cell Biol. 26 (2007) 577–587.
[35] C. Buske, M. Feuring-Buske, J. Antonchuk, P. Rosten, D.E. Hogge, C.J. Eaves, R.K. Humphries, Overexpression of HOXA10 perturbs human lymphomyelopoiesis in vitro and in vivo, Blood 97 (2001) 2286–2292.
[36] M. Iwata, Retinoic acid production by intestinal dendritic cells and its role in T-cell trafficking, Semin. Immunol. 21 (2009) 8–13.
[37] Y.C. Lin, S. Jhunjhunwala, C. Benner, S. Heinz, E. Welinder, et al., A global network of transcription factors, involving E2A, EBF1 and Foxo1, that orchestrates B cell fate, Nat. Immunol. 11 (2010) 635–643.
[38] T. Kanaitsuka, Y. Namba, Y.L. Zu, K. Ishii, T. Ashihara, M. Hanaoka, T. Suchi, Detection of fos oncogene products by monoclonal antibody FO-120 in lymphoproliferative disorders, Leuk. Res. 13 (1989) 1025–1033.
[39] G. Troen, V. Nygaard, T.K. Jenssen, I.M. Ikonomou, A. Tierens, et al., Constitutive expression of the AP-1 transcription factors c-jun, junD, junB, and c-fos and the marginal zone B-cell transcription factor Notch2 in splenic marginal zone lymphoma, J. Mol. Diagn. 6 (2004) 297–307.
[40] C.M. Annunziata, L. Hernandez, R.E. Davis, A. Zingone, L. Lamy, L.T. Lam, E.M. Hurt, A.L. Shaffer, W.M. Kuehl, L.M. Staudt, A mechanistic rationale for MEK inhibitor therapy in myeloma based on blockade of MAF oncogene expression, Blood 117 (2011) 2396–2404.
[41] U. Thorsteinsdottir, G. Sauvageau, M.R. Hough, W. Dragowska, P.M. Lansdorp, H.J. Lawrence, C. Largman, R.K. Humphries, Overexpression of HOXA10 in murine hematopoietic cells perturbs both myeloid and lymphoid differentiation and leads to acute myeloid leukemia, Mol. Cell. Biol. 17 (1997) 495–505.
[42] R.K. Gupta, Z. Arany, P. Seale, R.J. Mepani, L. Ye, H.M. Conroe, Y.A. Roby, H. Kulaga, R.R. Reed, B.M. Spiegelman, Transcriptional control of preadipocyte determination by Zfp423, Nature 464 (2010) 619–623.
[43] M. Francois, P. Richette, L. Tsagris, M. Raymondjean, M.C. Fulchignoni-Lataud, C. Forest, J.F. Savouret, M.T. Corvol, Peroxisome proliferator-activated receptor-gamma down-regulates chondrocyte matrix metalloproteinase-1 via a novel composite element, J. Biol. Chem. 279 (2004) 28411–28418.
[44] P. Delerive, F. Martin-Nizard, G. Chinetti, F. Trottein, J.C. Fruchart, J. Najib, P. Duriez, B. Staels, Peroxisome proliferator-activated receptor activators inhibit thrombin-induced endothelin-1 production in human vascular endothelial cells by inhibiting the activator protein-1 signaling pathway, Circ. Res. 85 (1999) 394–402.
[45] M.E. Gershwin, D.R. Lentz, R.S. Beach, L.S. Hurley, Nutritional factors and autoimmunity. IV. Dietary vitamin A deprivation induces a selective increase in IgM autoantibodies and hypergammaglobulinemia in New Zealand Black mice, J. Immunol. 133 (1984) 222–226.
[46] S.M. Smith, C.E. Hayes, Contrasting impairments in IgM and IgG responses of vitamin A-deficient mice, Proc. Natl. Acad. Sci. U. S. A. 84 (1987) 5878–5882.
[47] J.A. Carman, C.E. Hayes, Abnormal regulation of IFN-gamma secretion in vitamin A deficiency, J. Immunol. 147 (1991) 1247–1252.
[48] J.H. Chang, H.R. Cha, S.Y. Chang, H.J. Ko, S.U. Seo, M.N. Kweon, IFN-gamma secreted by CD103+ dendritic cells leads to IgG generation in the mesenteric lymph node in the absence of vitamin A, J. Immunol. 186 (2011) 6999–7005.